

A computational and experimental study on the Jahn-Teller effect in the hydrated copper (II) ion. Comparisons with hydrated nickel (II) ions in aqueous solution and solid Tutton's salts

This article has been downloaded from IOPscience. Please scroll down to see the full text article.

1989 J. Phys.: Condens. Matter 1 2395

(<http://iopscience.iop.org/0953-8984/1/13/012>)

View [the table of contents for this issue](#), or go to the [journal homepage](#) for more

Download details:

IP Address: 171.66.16.90

The article was downloaded on 10/05/2010 at 18:04

Please note that [terms and conditions apply](#).

A computational and experimental study on the Jahn–Teller effect in the hydrated copper(II) ion. Comparisons with hydrated nickel(II) ions in aqueous solution and solid Tutton's salts

B Beagley[†], A Eriksson[‡], J Lindgren[‡], I Persson[§], L G M Pettersson^{||}, M Sandström^{¶††}, U Wahlgren^{||} and E W White[†]

[†] Department of Chemistry, UMIST, PO Box 88, Manchester M60 1QD, UK

[‡] Institute of Chemistry, University of Uppsala, PO Box 531, S-751 21 Uppsala, Sweden

[§] Inorganic Chemistry 1, Chemical Center, University of Lund, PO Box 124, S-221 00 Lund, Sweden

^{||} Institute of Theoretical Physics, University of Stockholm, Vanadisvägen 9, S-113 46 Stockholm, Sweden

[¶] Department of Inorganic Chemistry, Royal Institute of Technology, S-100 44 Stockholm, Sweden

Received 24 October 1988

Abstract. *Ab initio* SCF molecular orbital calculations have been performed on the free $\text{Cu}(\text{OH}_2)_6^{2+}$ complex in D_{2h} symmetry. Two extrema in the adiabatic electron energy potential surface were obtained corresponding to a tetragonal distortion from the regular T_h symmetry of the octahedral complex, as expected from the Jahn–Teller theorem in a case with strong E–e type vibronic coupling. The tetragonally elongated octahedral structure with Cu– $2O_{ax}$ at 2.25 Å and Cu– $4O_{eq}$ at 2.06 Å gave a slightly lower energy (72 cm^{-1}) than the compressed geometry with Cu– $2O_{ax}$ at 2.02 Å and Cu– $4O_{eq}$ at 2.17 Å. The calculated Jahn–Teller energy is 650 cm^{-1} from that of the regular T_h symmetry with Cu–6O at 2.115 Å. EXAFS measurements were performed on aqueous Cu^{2+} solutions and showed a greater distortion with Cu– $4O_{eq}$ at 1.99 Å and Cu– $2O_{ax}$ at about 2.29 Å. Infrared absorption spectroscopic measurements were made on the O–D stretching vibrations of HDO molecules in aqueous Cu^{2+} and Ni^{2+} solutions with added D_2O in order to study the hydrogen bonds from the hydrated ions. A distorted $\text{Cu}(\text{OH}_2)_6^{2+}$ ion is expected to form hydrogen bonds of unequal strength because of the stronger polarisation of the more strongly bonded equatorial water molecules. Two bands ascribed to the hydration of the Cu^{2+} ion were obtained, the more intense corresponding to the strongest hydrogen bonds at $\approx 2400\text{ cm}^{-1}$, and the weaker at $\approx 2530\text{ cm}^{-1}$, whereas for Ni^{2+} only one band at $\approx 2420\text{ cm}^{-1}$ was found. With the use of a correlation between $R_{O\cdots O}$ versus ν_{OD} from crystal structure data the mean hydrogen-bonded O \cdots O distances to the second hydration shell are estimated to about 2.74 Å from the equatorial water molecules and 2.88 Å from the axial. The IR data show that the distortions induced by the Jahn–Teller effect on the second hydration sphere are visible on a vibrational timescale, despite the fast intramolecular inversion of the distortion axis between the three principal octahedral directions. The splitting of the ν_{OD} bands in the Tutton salts $\text{C}_2\text{S}_2[\text{M}(\text{OH}_2)_6](\text{SO}_4)_2$, M = Cu or Ni, with some added D_2O has also been measured and compared to crystal structure data of the hydrogen bonded distances. The separation of about 107 cm^{-1} between the two groups of O–D stretching vibrations found in the Cu salt can be ascribed to a static Jahn–Teller effect.

†† Author to whom correspondence should be addressed.

1. Introduction

The Jahn–Teller theorem has great practical importance in understanding the structural, spectroscopic and dynamic properties of many transition metal complexes [1]. The octahedral complexes of the divalent ion copper(II) with nine d electrons in the valence shell with the configuration $(t_g)^6, (e_g)^3$, constitute classical examples of Jahn–Teller systems with strong vibronic coupling for which quasi-stationary distortions in the nuclear configuration separated by small energy barriers, can be obtained [1, 2]. An octahedral Cu(II)–O₆ entity with O_h symmetry is a Jahn–Teller system with configurational instability of the fundamental E–e type (coupling with the e_g-type vibration) [1, 2]. Although the instability is caused by vibronic couplings, the adiabatic approximation will be fulfilled at stable nuclear configurations, provided that the spacing of the e_g vibrational energy levels is small compared with the splitting of the electronic terms. The highest symmetry of the Cu(OH₂)₆²⁺ complex is T_h when all bonds are equal, figure 1. The Jahn–Teller active e_g vibration lowers the symmetry to D_{2h} and gives a ²A_g ground state. Since the additional perturbation induced by the hydrogen atoms from the O_h symmetry of a CuO₆ octahedron is rather weak, the analyses by means of a tetragonal distortion of the octahedral case will give the essential features for a hydrated Cu²⁺ ion in the gas phase. If the energy of the system is calculated in the adiabatic approximation by including vibronic couplings through first-order perturbation theory for the symmetrical configuration, the potential surface takes the form of the well known ‘Mexican hat’ if only linear terms are used, figure 2(a). If also quadratic terms in the vibronic interactions are included the surface becomes warped (figure 2(b) ([1]; see also Ch. 2 and 3 in [2])). The minima along the valley in the warped ‘Mexican hat’ adiabatic potential (AP) surface correspond to tetragonally elongated configurations and the maxima (saddle points) to tetragonally compressed configurations with the e_g orbitals d_{x²–y²} and d_{z²} of the Cu²⁺ ion singly occupied, respectively. The depth of the minima from the regular octahedral structure is the Jahn–Teller energy E_{JT}, and the barrier height between the minima is denoted 2β.

For the Cu(OH₂)₆²⁺ complex in solution the barrier has been found high enough to give the transitions from one deformation of the octahedron to another the character of

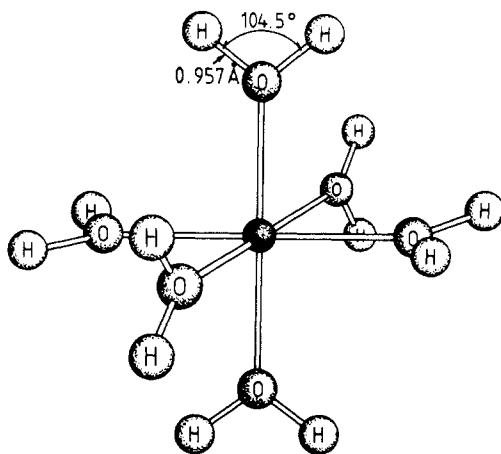


Figure 1. The [Cu(OH₂)₆]²⁺ complex in T_h symmetry.

Bek†

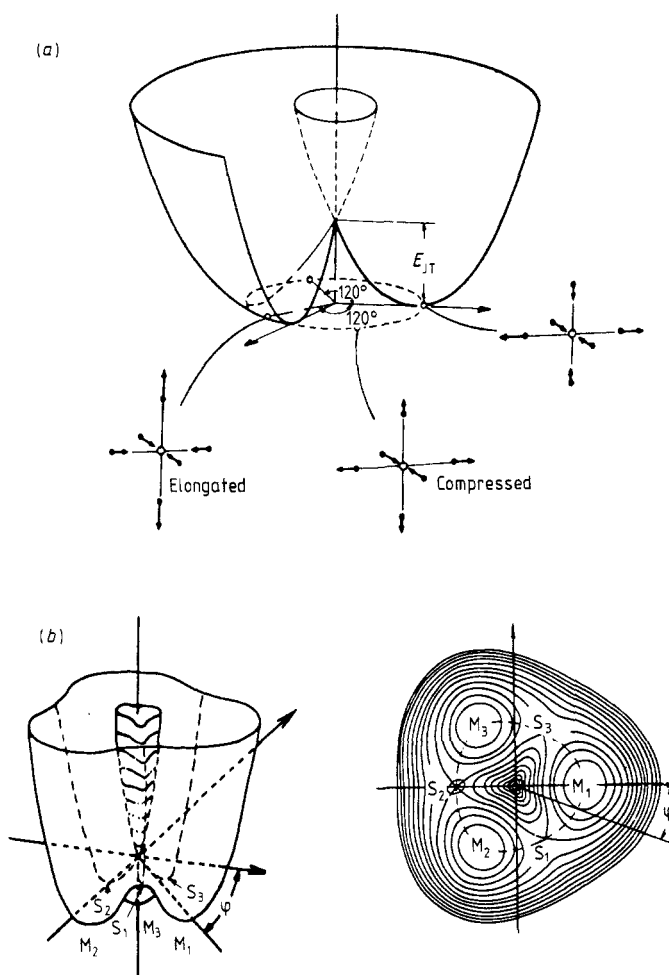


Figure 2. (a): The 'Mexican hat' adiabatic potential of an octahedral system ML_6 in the linear $E-e$ case. The distortions of the octahedron varies continuously in D_{2h} symmetry along the bottom of the trough from tetragonally elongated to compressed configurations (see [1], figure 2.5); (b): The warped Mexican hat AP surface with three minima M_1 to M_3 , and three saddle points, S_1 to S_3 (see [1], figure 2.2).

pulsations changing the direction of distortion to another equivalent configuration [3], with a much lower frequency than for the e_g vibrations.

For the $Cu(OH_2)_6^{2+}$ octahedron incorporated in a crystal lattice another effect has to be considered in the Hamiltonian. External low-symmetry fields will cause an additional warping of the 'Mexican hat' AP surface leading to non-equivalent minima, which will emphasise a certain direction of the distortion [1, 2, 4].

The purpose of the present study was firstly to investigate the effect of the Jahn–Teller induced splitting of the degenerate electronic states in an isolated $Cu(OH_2)_6^{2+}$ cluster by a theoretical calculation. Secondly, the perturbation and enhancement of the effect in condensed systems by the surrounding was studied experimentally, in particular the role of the hydrogen bonds. We have performed *ab initio* SCF calculations to find the

minima in the two intersecting sheets of the adiabatic energy potential for singly occupied d_{z^2} and $d_{x^2-y^2}$ orbitals of the Cu(II) ion, respectively. The 'Mexican hat' AP surface results from the mixing of these two electronic states. The magnitude of the distortions corresponding to these minima was estimated assuming that the nuclear motion could be described by the AP surface. In order to compare the calculated Cu–O distances with experimental values in condensed phases, we made EXAFS measurements on aqueous solutions of Cu^{2+} ions with different anions at varying concentrations. Hydrogen bonds formed to strongly bonded and polarised aqua ligands should be stronger than those formed to the more loosely bonded water molecules. In order to investigate this effect on the first hydration shell of the $\text{Cu}(\text{OH}_2)_6^{2+}$ octahedron we performed infrared spectroscopic studies of the hydrogen bonds formed from the hydration shell around Cu^{2+} ions in aqueous solution and in the Tutton salt $\text{Cs}_2[\text{Cu}(\text{OH}_2)_6](\text{SO}_4)_2$, and compared these with the corresponding Ni^{2+} spectra.

2. Previous studies

Jahn–Teller distorted hydrated copper(II) ions have been extensively studied both in solid state and in solution [1–19].

The temperature dependence of the g -values from ESR studies of the Cu^{2+} ion doped into Tutton's salts, for example, in a $\text{Cs}_2[\text{Zn}(\text{OH}_2)_6](\text{SO}_4)_2$ lattice, was interpreted in a previous investigation with distributions over energy levels corresponding to different orientations of the $\text{Cu}(\text{OH}_2)_6^{2+}$ ions in the host lattice [6]. This model has also been used to explain low-temperature crystallographic studies on the variations in the geometry of $[\text{Cu}(\text{OH}_2)_6]^{2+}$ ions in the pure copper Tutton's salts in terms of a temperature-dependent fluxional behaviour of approximately tetragonally elongated octahedral CuO_6 entities, aligned in different directions [7]. The validity of this approach was questioned in a later study because of the cooperative interactions expected in a pure compound [4]. Careful X–N electron density studies of the Tutton salts $(\text{NH}_4)_2[\text{M}(\text{OH}_2)_6](\text{SO}_4)_2$, with $\text{M} = \text{Cu}, \text{Mg}$ or Ni , have shown that strong hydrogen bonding of the coordinated water molecules will increase the strength of the M–OH_2 bonds [8].

In solution, several diffraction and EXAFS studies have been performed on the hydrated Cu^{2+} ion. Concentrated (1.9 and 2.9 mol l^{-1}) aqueous $\text{Cu}(\text{ClO}_4)_2$ solutions were studied by x-ray diffraction [9] and four Cu–O_{eq} distances were found at 1.98 \AA . The axial distances Cu–O_{ax} 2.39 and 2.34 \AA , respectively, were reported, although the determination is difficult due to the weaker bonding and the overlap with the O–O distances within the ClO_4^- ion. A previous x-ray diffraction study on a 3.6 mol l^{-1} $\text{Cu}(\text{ClO}_4)_2$ solution gave for Cu–O_{eq} and Cu–O_{ax} 1.94 \AA and 2.43 \AA , respectively [10]. For 1.4 mol l^{-1} CuSO_4 solutions the corresponding distances 1.94 and 2.38 \AA [11], and 2.00 and 2.33 \AA [12], respectively, were obtained.

EXAFS data on the K-absorption edge of Cu give scattering curves which do not contain contributions from anions or water structure. Due to the inherent limitations in the k -space data range which can be obtained with this technique, and the interference effects between the two close Cu–O distances [13], the axial bond lengths with a larger variation about their mean distance, are still difficult to determine. From three different studies on $\text{Cu}(\text{ClO}_4)_2$ solutions the Cu–O_{eq} distances were found to be 2.00 , 1.94 and 1.96 \AA , while the values 2.28 , 2.46 , and 2.60 \AA were given for Cu–O_{ax} , respectively [13–15]. Recently, however, an EXAFS study was reported of vitreous glassy $\text{Cu}(\text{ClO}_4)_2$ solutions with concentrations from 0.3 to 3.4 mol l^{-1} at liquid nitrogen temperature [16].

Both the mean Cu–O_{eq} and Cu–O_{ax} bond lengths were found to be constant, 1.96 and 2.3 Å, respectively. Only the variation of the axial distance was found to increase slightly with increasing concentration.

Also with the use of neutron diffraction methods, elimination of the solvent background can be achieved by isotopic or isomorphous difference methods [17]. An isomorphous study on a 3.8 mol l⁻¹ Cu(ClO₄)₂ solution in D₂O resulted in two broad peaks in a radial distribution curve which were ascribed to Cu–O distances at 1.97 Å and Cu···D at 2.60 Å in a Cu(OD₂)₆²⁺ ion [18]. The resolution was rather low, however, and no conclusions about two different Cu–O distances could be drawn. Another subsequent difference study on 2 molal (mol kg⁻¹) Cu(ClO₄)₂ solutions prepared using the isotopes ⁶³Cu and ⁶⁵Cu, respectively, again gave two major peaks, albeit with a somewhat better resolution [19]. The first peak was found to correspond to 4.1 Cu–O distances at 1.96 Å, but due to the overlapping Cu–O_{ax} and Cu···D distances in the second peak centred at 2.6 Å, no conclusions were drawn on the detailed hydration structure [19].

Kinetic data on dilute Cu²⁺ solutions [3] show that the water exchange rate is much faster for Cu²⁺ than for most other divalent metal ions [20]. A combination of ESR and NMR results gave a mean residence time of about 2 × 10⁻¹⁰ s for inner shell water oxygen atoms in the complex, and the lifetime between the intramolecular inversions from one equivalent elongation of the Cu(OH₂)₆²⁺ complex to another, was estimated to about 10⁻¹¹ s [3]. A recent quasi-elastic neutron scattering (QENS) experiment, measuring the translational diffuse motion of protons in 2 and 3 molar Cu(ClO₄)₂ solutions, showed no evidence for non-equivalent water protons on the timescale of the QENS experiment, ≈10⁻¹⁰ s [21]. This was, however, found for the Ni²⁺ ion with a corresponding cation–water proton binding time longer than ≈5 × 10⁻⁹ s [21].

The combined experimental structural evidence thus is consistent with a ‘static’ tetragonally elongated octahedral configuration of the Cu(OH₂)₆²⁺ complex on the timescale of diffraction or EXAFS interactions in condensed phases. From early crystal field arguments a tetragonal compression with two shorter Cu–L distances of a CuL₆ cluster was expected to give lower energy than an elongation [22]. Later, the experimentally found preference for an elongated structure for free Cu(OH₂)₆²⁺ clusters has been proposed to result from configuration interactions with the lowest excited states, [23] and by 3d_{z²}–4s mixing [24]. A subsequent *ab initio* MO calculation gave, however, the same Jahn–Teller energy E_{JT} for the minima corresponding to a tetragonally elongated and a compressed structure, respectively [25]. This value, 440 cm⁻¹, is much smaller than the experimental E_{JT} energy as estimated for a number of Cu(II)–O₆ octahedra, about 1810 cm⁻¹ (ch 13 in [2]). Since the frequency of the Jahn–Teller active e_g vibration has been estimated to $h\nu = 254(27)$ or 300 cm⁻¹ (ch 13 in [2], [4]), this confirms that the experimental system represents a case with strong vibronic coupling because $E_{JT} \gg h\nu$ [1].

3. Theoretical calculation

3.1. Method

The quantum chemical study of the free Cu(OH₂)₆²⁺ cluster was performed at the SCF level of approximation using the MOLECULE-ALCHEMY program system [26]. Since the inner shells, Cu(1s, 2s, 2p) and O(1s), are expected to retain their atomic properties

they were replaced by effective core potentials (ECP) [26, 27], which accurately reproduce the interaction between the core and valence electrons. The Cu(3s, 3p) orbitals were kept frozen to improve the ECP description further, while the orbital determination for the 4s and 3d electrons are fully variational. This approach has been demonstrated [26, 27] to give results in complete agreement with those obtained using the basis set from which the ECP was developed but at a substantially lower computational expense. The Cu basis set used is equivalent to that suggested by Roos *et al* [28] with two additional diffuse p functions and an additional diffuse d function. The oxygen basis set, and also the ECP, [29] is based on the triple-zeta type basis of Huzinaga [30] and contains an additional diffuse p function to account for O⁻ character. The hydrogen basis finally, is the Huzinaga 4s basis [30] contracted to 2s with the exponents scaled by a factor 1.25 to allow for the reduced electronic charge on H in the H₂O molecule. The internal H₂O geometry was fixed at the experimental value in gas phase [31] (O–H 0.957 Å, H–O–H 104.5°) at all points.

The distortion of the T_h symmetry of the Cu(OH₂)₆²⁺ complex was described by a symmetrical elongation or compression of two opposite Cu–O_{ax} distances, corresponding to Cu²⁺ states with singly occupied d_{x²-y²} and d_{z²} orbitals, respectively. The effects due to the different orientations between the axial and the two pairs of equatorial water molecules were neglected, and the four Cu–O_{eq} distances were kept equal.

3.2. Results

Two energy extrema in the AP surface were obtained for the configurations Cu–4O_{eq}, Cu–2O_{ax}: 2.057, 2.250 Å (elongated) and 2.172, 2.024 Å (compressed), respectively. The elongated geometry, which has the slightly lower energy, corresponds to the troughs in a warped ‘Mexican hat’ AP surface, and the compressed configuration to the saddle points, Fig. 2b. The calculated energy difference 2β is found to be only 72 cm⁻¹ (0.86 kJ mol⁻¹). The experimental value 2β for a barrier separating quasi-stationary states with a lifetime of 1.6 × 10⁻¹¹ s, however, has been estimated to 5.0 kJ mol⁻¹ at 25 °C in aqueous solution [3].

The regular structure in T_h symmetry was found to have its lowest energy for a Cu–O distance of 2.115 Å, with the calculated Jahn–Teller energy E_{JT} = 650 cm⁻¹ (7.8 kJ mol⁻¹) over the minimum for the elongated structure. It is obvious that the calculated barriers, both E_{JT} and 2β, for the isolated [Cu(OH₂)₆]²⁺ complex are much lower than the experimental values. This may mainly be a result of the hydrogen bonding in the condensed phases, which is expected to further stabilise the tetragonally elongated configuration and increase the depth of the minima, as discussed in § 5. However, even though effects from configuration interactions are expected to be small in this type of ionic systems, they may give some contribution especially to the calculated barriers. These effects have not been estimated in the present calculation.

The calculated geometrical distortion, as given by the minima of the AP surface, is also smaller than in solution. The Jahn–Teller radius (ch 13 in [2]), R_{JT} = (ΣΔR_i²)^{1/2}, is 0.22 Å for the calculated values for the elongated configuration. The mean experimental value for the EXAFS results on the Cu(NO₃)₂ solution in table 1 is 0.33 Å (see also table 12a, in ch 13 of [2]). This is probably also an effect of the additional perturbation by the hydrogen bonds, which not only increases the depth of the minima but may also shift the position of the troughs in the AP, see figure 2(b). The criterion for strong vibronic coupling, ensuring that there is a physical basis for assuming the nuclear motion to be controlled by the AP surface is still fulfilled, however [1; see also ch 13 in

Table 1. Structure parameters obtained by EXAFS for hydrated Cu^{2+} ions. Four equatorial and two axial Cu–O distances R (in Å) have been assumed. The σ_j^2 parameter (Å^2) in the Debye–Waller factor $\exp(-2\sigma_j^2 k^2)$ corresponds to the mean-square deviation from the mean distance R [36], but is coupled to the assumed value for the calibration compound $\text{CuSO}_4 \cdot 5\text{H}_2\text{O}$ [37]. The estimated errors from the fitting procedures are given within parentheses.

Sample	R_{eq}	σ_{eq}^2	R_{ax}	σ_{ax}^2	Reference†
$\text{CuSO}_4 \cdot 5\text{H}_2\text{O}$	1.956 (fix)	0.013	2.43(2)	$= \sigma_{\text{e}}^2$	This work ^a
CuSO_4 (1.3 M)	2.00 (2)	0.012	2.27 (3)	$= \sigma_{\text{e}}^2$	This work ^a
CuSO_4 (0.5 M)	2.00 (3)	0.0092	2.27 (3)	$= \sigma_{\text{e}}^2$	This work ^a
$\text{Cu}(\text{NO}_3)_2$ (0.2 M)	2.04 (1)	0.0055	2.29 (1)	$= \sigma_{\text{e}}^2$	This work ^a
$\text{Cu}(\text{NO}_3)_2$ (0.2 M)	1.99 (2)	0.0055	2.28 (5)	0.022	This work ^b
$\text{Cu}(\text{NO}_3)_2$ (0.2 M)	1.99 (2)	0.002	2.31 (5)	0.007	This work ^c
$\text{Cu}(\text{ClO}_4)_2$ (1.0 M)	2.00 (1)	0.0036	2.28 (5)	0.011	[13]
$\text{Cu}(\text{ClO}_4)_2$ (1.0 M)	1.96 (1)	0.0013	2.60 (5)	0.015	[15]
$\text{Cu}(\text{ClO}_4)_2$ (0.3 M)	1.96	0.004	2.3	0.020	[16]

† The different program systems used for the data evaluation are described in: ^a [35], ^b [33] and ^c [34].

[2]), since the calculated energy difference between the two states having a singly occupied d_{z^2} and $d_{x^2-y^2}$ orbital is approximately 2470 cm^{-1} at the energy minima, i.e. $\sim 4 E_{\text{JT}}$ [1, 2].

The previous MO calculation gave a still smaller tetragonality with Cu– O_{eq} 1.96 and Cu– O_{ax} 2.06 Å for the elongated structure, and Cu– O_{eq} 2.02, Cu– O_{ax} 1.94 Å for the compressed [25]. However, due to the low quality of the basis sets used these results should be viewed with caution. In the present investigation substantially improved basis sets were used, which allow greater flexibility in the valence regions and also smaller basis set superposition errors than those expected from the minimal basis set calculation of [25].

4. EXAFS measurements

4.1. Method

X-ray Cu K-edge absorption data were collected with the use of the EXAFS facilities at the synchrotron radiation source (SRS) at Daresbury Laboratory as described in [32]. Transmission geometry was used for the nitrate solution and fluorescence mode was used for the other samples, table 1. The transmission data were treated using the EXAFS program system in the SRS library (EXCURVE) [33], and also using the two different software packages developed at the University of Illinois (XFPACK) [34], and at UMIST [35], in order to compare the effects of the different procedures for calibrations and corrections used. For the fluorescence data only the UMIST software was used. In the data treatment a model with four short and two long Cu–O distances was used. Models with six equal or four long and two short distances were also tested but gave poorer fits. The four short distances dominate the scattering strongly which makes the determination of the two long distances less reliable.

4.2. Results

The results are summarised in table 1. They support the previous conclusions that the average solution structure of the hydrated Cu^{2+} ion is a distorted octahedron with four short and two longer Cu–O distances. No significant influence of the anions is seen. The Debye–Waller factors are directly coupled to the values chosen for the calibration compound and are also sensitive for errors in the background elimination procedures, and should here be regarded as fitting parameters which are difficult to compare between different investigations and calibrations. The measurements made in fluorescence mode on the CuSO_4 solutions can be regarded as exploratory, and the most reliable values are those obtained for the $\text{Cu}(\text{NO}_3)_2$ solution. The mean of the values obtained by the use of the EXCURVE and XPAK programs, where the two Debye–Waller factors were independently varied, is chosen, i.e. Cu–O_{eq} 1.99(2) and Cu–O_{ax} 2.29(5) Å.

5. Infrared spectroscopy

5.1. Method

The hydration of ions in moderately concentrated aqueous solutions ($>0.1 \text{ mol l}^{-1}$) has been studied by IR absorption spectroscopy using a double-difference technique developed by Lindgren and co-workers [38, 39]. The wavenumbers of the O–D stretching vibrations of isotopically isolated HDO molecules were used as a measure of the various interactions in which a water molecule could participate. This wavenumber is known to decrease with increasing hydrogen bond strength. A water molecule directly bonded to a cation (by an ion–dipole interaction) is polarised by that cation; a stronger polarisation makes the water molecule a better hydrogen bond donor. The water molecule–ion distance and the charge of the ion are important factors for the magnitude of this polarisation.

Several divalent cations (Mg^{2+} , Mn^{2+} , Fe^{2+} , Ni^{2+} and Zn^{2+}), believed to coordinate six water molecules octahedrally in their first hydration sphere in solution [17, 20], were shown to give a single well defined O–D stretching absorption band at $\approx 2420 \text{ cm}^{-1}$, a relatively low wavenumber which indicates a substantial polarising influence from the cation on the coordinated water molecules in its first hydration shell [38, 39].

5.2. Solution results

The two spectra in figure 3, for 0.5 M $\text{Ni}(\text{ClO}_4)_2$ and for 0.5 M $\text{Cu}(\text{ClO}_4)_2$, are scaled for six water molecules in the first hydration shell of the cations [39]. In the case of the Cu^{2+} ion in solution, two broad absorption bands which can be ascribed to O–D stretchings from its water of hydration appear in the IR spectrum, but there is only one corresponding band for the Ni^{2+} solution, table 2. A distortion of the hydration layer around the Cu^{2+} ion by the Jahn–Teller effect, making the water molecules in the first hydration shell unequivalent with respect to Cu–O distances, polarisation, hydrogen–bond donor properties and O–D stretching wavenumbers, is the probable reason for the observations. The more intense band (figure 3) at 2400 cm^{-1} would then correspond to the hydrogen bonds formed with the more strongly bonded equatorial water molecules, while the weaker band at 2530 cm^{-1} should be caused by the axial water molecules. With the use of an equation, obtained from solid-state correlations between hydrogen-bonded oxygen atoms $R_{\text{O}\dots\text{O}}$, and ν_{OD} wavenumbers [41], hydrogen-bond distances can be estimated

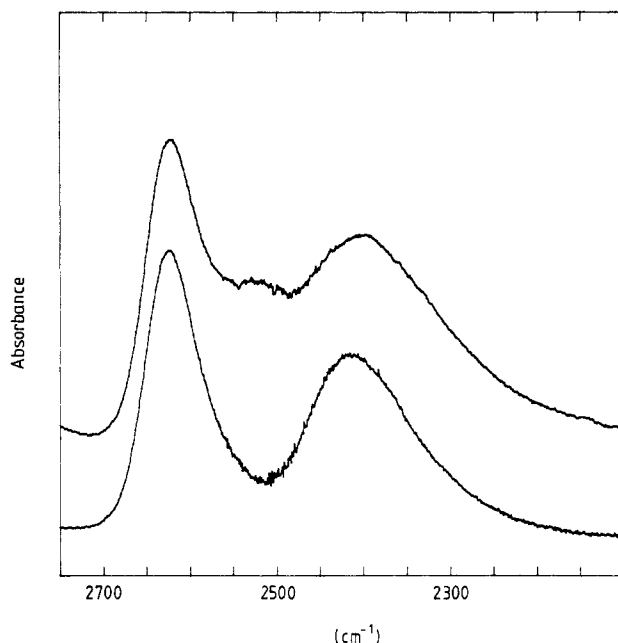


Figure 3. Infrared absorption spectra (path length 0.050 mm, 293 K) of 0.5 M aqueous solutions (8 mol% HDO) of $\text{Cu}(\text{ClO}_4)_2$ (upper curve) and $\text{Ni}(\text{ClO}_4)_2$ (lower curve), obtained using the double difference technique described in [38, 39]. The pH of the $\text{Cu}(\text{ClO}_4)_2$ solution was 3.4 (to avoid the formation of hydroxo complexes) and around 5 for the $\text{Ni}(\text{ClO}_4)_2$ solution. The absorption bands at $\approx 2623 \text{ cm}^{-1}$ emerge from the hydration of the ClO_4^- ion [38, 39]; the other bands are discussed in the text.

Table 2. Infrared O \leftrightarrow D stretching frequencies (wavenumbers in cm^{-1} of band maxima) of HDO molecules bonded to ions in aqueous solution, and the corresponding derived O \cdots O hydrogen-bonded distances in Å [41].

Interaction	O \leftrightarrow D stretch	O \cdots O distance	Reference
$\text{Cu}^{2+}\text{-O} \leftrightarrow \text{D} \cdots \text{O}$	2400, 2530	2.74, 2.88	This work
$\text{Ni}^{2+}\text{-O} \leftrightarrow \text{D} \cdots \text{O}$	2420	2.76	[38, 39]
$\text{H-O} \leftrightarrow \text{D} \cdots \text{O}$ (water)	2506	2.86	[38]
$\text{O}_3\text{ClO}^- \cdots \text{D} \leftrightarrow \text{O-H}$	2623	3.05	[39]

from the equatorial and axial water oxygen atoms to the second shell of hydration. The corresponding O \cdots O distances for the ClO_4^- and Ni^{2+} ions [38, 39] are also given for comparison, table 2.

5.3. Solids

In order to support the conclusions made for the solution spectra it is of interest to compare experimental results for $\text{Cu}(\text{OH}_2)_6^{2+}$ and $\text{Ni}(\text{OH}_2)_6^{2+}$ complexes in the solid state. For example, in the isomorphous Tutton salts, $\text{Cs}_2[\text{M}(\text{OH}_2)_6](\text{SO}_4)_2$, with $\text{M} = \text{Cu}$ or Ni , the $\text{Ni}(\text{OH}_2)_6^{2+}$ complex has a fairly regular octahedral Ni-O_6 symmetry, while

Table 3. Comparison of some distances (Å) and angles (°) with some estimated standard deviations within parentheses from crystal structure investigations of the Tutton's salts $(M')_2[M(OH_2)_6](SO_4)_2$. The differences $\Delta_{NH_4}(D-P)$, in the bond lengths between the deuterated [44] and the protonated [7] ammonium salts at 123 K show the correlation between the changes in the Cu–O and O···O bond lengths (the dots denote hydrogen bonds). The cesium salts were investigated at ambient temperatures [42, 43]. The maximum difference between x-ray and neutron diffraction studies for the distances quoted in the table (due to electron density polarisations) is 0.014 Å for Cu–O (7) in the $(NH_4)_2[Cu(OH_2)_6](SO_4)_2$ salt at 295 K [8]. This gives an estimate of the upper limit of the systematic errors in the comparison between corresponding distances in the cesium and ammonium salts.

M'	Cs ^a	Cs ^b	ND ₄ ^b	NH ₄ ^a	$\Delta_{NH_4}(D-P)$
M	Ni	Cu	Cu	Cu	
M–O (7)	2.070 (3)	2.004 (4)	2.006 (4)	2.278 (2)	–0.272
O (7)···O (5)	2.737 (4)	2.714	2.744	2.842	–0.098
O (7)···O (6)	2.796 (4)	2.722	2.778	2.833	–0.055
M–O (8)	2.086 (2)	2.315 (5)	2.318 (5)	2.012 (1)	0.306
O (8)···O (4)	2.715 (4)	2.780	2.764	2.683	0.081
O (8)···O (6)	2.746 (4)	2.782	2.826	2.725	0.101
M–O (9)	2.046 (2)	1.966 (5)	1.950 (4)	1.970 (1)	–0.020
O (9)···O (3)	2.682 (4)	2.702	2.701	2.681	0.020
O (9)···O (5)	2.762 (4)	2.706	2.711	2.730	–0.019
O (5)···O (7)···O (6)	116.8 (1)	114.6	111.0	119.9	
O (4)···O (8)···O (6)	99.5	101.1	102.3	105.6	
O (3)···O (9)···O (5)	94.4	97.6	104.6	97.3	

^a X-ray diffraction

^b Neutron diffraction

the $Cu(OH_2)_6^{2+}$ complex is tetragonally elongated, table 3 [42, 43]. Each water molecule is hydrogen bonded to two sulphate oxygen atoms, figure 4.

The IR absorption bands from OD-stretching vibrations of isotopically isolated HDO molecules in the Cu and Ni salts are shown in figure 5. The overall spectral features are similar at 300 K and 100 K although the bands are much narrower at the lower temperature and therefore better resolved.

In the caesium salt, $Cs_2[Cu(OH_2)_6](SO_4)_2$, the O(8) water oxygen atoms, which are involved in the long Cu–O(8) bond (table 3), also have longer O···O (and H···O) [42] hydrogen bonds. From the series of crystal structures of Tutton's salts and the variation of EPR parameters with temperature [4, 6, 44], it seems that at least at low temperature the $Cu(OH_2)_6^{2+}$ octahedra are ordered with respect to the direction of the elongated axis.

From the correlation between O–D-stretching wavenumbers and O···O hydrogen bond distances [41], it is clear that the two longest O···O bonds (2.782 and 2.780 Å) correspond to the two highest O–D wavenumbers (2478 and 2461 cm^{-1}) in the uppermost curve of the IR spectra in figure 5. The other three (four expected, overlap) observed bands at lower wavenumbers (2392, 2360 and 2339 cm^{-1}) are then assigned as O–D-stretching vibrations of the equatorial water molecules involved in the shorter hydrogen bonds, table 3. The splitting between the two groups of bands in the IR spectrum (figure

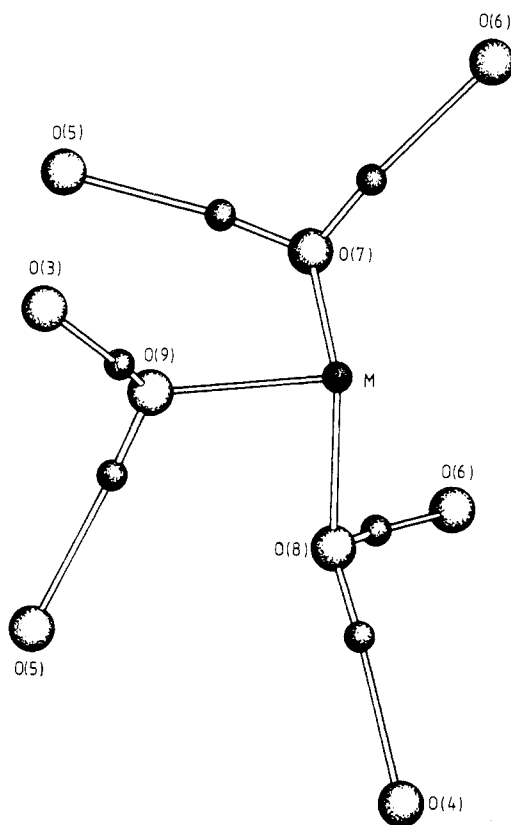


Figure 4. The metal–oxygen coordination and hydrogen bonds in the octahedral $[M(OH_2)_6]^{2+}$ complexes in the Tutton salts $Cs_2[M(OH_2)_6](SO_4)_2$, $M = Cu$ or Ni [42, 43], with parameters from the Cu structure. Only one side of each centrosymmetrical pair of atoms is shown for clarity. The oxygen atoms $O(3)$ to $O(6)$ belong to sulphate groups.

5) is about 107 cm^{-1} . The mean values of their wavenumbers give, using the correlation in [41], a mean $O(8)_{ax} \cdots O$ hydrogen bond distance of 2.80 \AA and an $O_{eq} \cdots O$ distance of 2.71 \AA . These values are in satisfactory agreement with the mean of the corresponding distances from the crystal structure determination, 2.78 and 2.71 \AA [42].

For the $Cs_2[Ni(OH_2)_6](SO_4)_2$ salt, the O–D-stretching IR absorption bands are less separated than for the Cu salt (figure 5), although the spread of the $O \cdots O$ distances is approximately the same, table 3. Following the correlations [41], it is clear that the pattern of O–D bands has also been mixed compared with those of the Cu salt. The situation is thus somewhat complicated, and unambiguous assignments on the basis of the $O \cdots O$ distances alone do not seem possible. We can note, however, that the elongation of the $[Cu(OH_2)_6]^{2+}$ octahedron in the Cs salt, and also for all other investigated alkali metal and copper Tutton's salts [6], occurs in the direction of the longest bond between metal to oxygen, $M-O(8)$, in the $[Ni(OH_2)_6]^{2+}$ complex, table 3. For the $Cs_2[Cu(OH_2)_6](SO_4)_2$ salt, we can therefore conclude that the effect of the Jahn–Teller distortion is to impose a splitting of the two groups of O–D stretchings with at least 100 cm^{-1} on top of the separations caused by the lattice effects.

When the Cs^+ ion is replaced with NH_4^+ another set of hydrogen bonds is introduced in the structure [8, 45]. Even though the $M-O(7)$ and $M-O(8)$ bonds are of about the

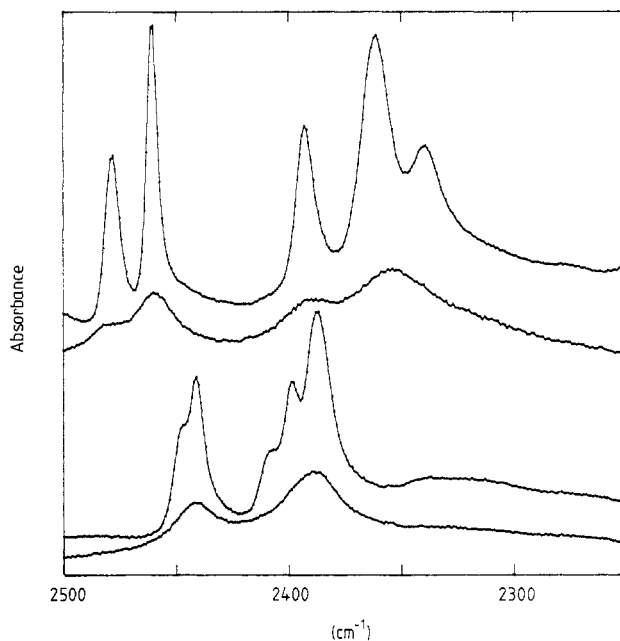


Figure 5. Infrared absorption spectra at 100 K (high-resolution curves) and 300 K in the O–D stretching region of powdered crystalline samples of $\text{Cs}_2\text{Cu}(\text{SO}_4)_2 \cdot 6(\text{H}, \text{D})_2\text{O}$ (upper spectra) and $\text{Cs}_2\text{Ni}(\text{SO}_4)_2 \cdot 6(\text{H}, \text{D})_2\text{O}$ (lower spectra). The molar ratio H/D is about 20 in both cases. The samples were prepared as mulls in fluorolube oil.

same length in all three $(\text{NH}_4)_2[\text{M}(\text{OH}_2)_6](\text{SO}_4)_2$ salts with $\text{M} = \text{Mg}, \text{Ni}$ or Zn [8, 46, 47], small changes in the hydrogen-bond strength seem to be sufficient to make the Cu–O(7) bond, instead of the Cu–O(8) as in the alkali metal salts, expand under the influence of the Jahn–Teller effect in the $(\text{NH}_4)_2[\text{Cu}(\text{OH}_2)_6](\text{SO}_4)_2$ compound [7, 8]. This sensitive balance is also made evident by a neutron powder diffraction study at different temperatures of the deuterated compound $(\text{ND}_4)_2[\text{Cu}(\text{OD}_2)_6](\text{SO}_4)_2$, for which again the Cu–O(8) bond is the longest [5, 44]. In table 3 a comparison of some of the distances in the structures is made at 123 K, a temperature for which thermally induced effects on the Cu–O bond lengths by a distribution of the elongated octahedra in different directions are expected to be small [7, 42]. This remarkable example of how an isotopic substitution can cause a profound change in the structure of a compound also clearly shows the relationship between the increase in length of a Cu–O bond and in the corresponding $\text{O} \cdots \text{O}$ hydrogen bonds from the water molecules coordinated to the copper atom, table 3. It is also clear from this comparison that the longest M–O bond length does not necessarily correspond to the longest hydrogen-bonded $\text{O} \cdots \text{O}$ distance, because of the lattice perturbations. In the absence of more detailed structure data, in particular accurate hydrogen atom positions, the M–O distances in the Tutton’s salts are therefore not sufficient indicators to make unambiguous assignments of hydrogen bond stretching frequencies.

6. Conclusions

The lowest energy in the AP surface for an isolated $\text{Cu}(\text{OH}_2)_6^{2+}$ cluster in D_{2h} symmetry was obtained for a tetragonally elongated T_h system, although the energy difference 2β

to the compressed configuration was only 72 cm^{-1} . The calculated energy values, E_{JT} and 2β , are smaller than the experimental in condensed systems, as well as the magnitude of the tetragonal elongation. The EXAFS results show a difference between the axial and equatorial Cu–O distances of about 0.3 \AA in aqueous solution, compared with the theoretically calculated value of 0.2 \AA .

However, IR absorption spectra of the O–D-stretching vibrations in solution show that the hydrogen bonds between the first and second hydration shells are of unequal strength and will give an additional contribution to the tetragonal elongation. The IR solution spectra also show that the Jahn–Teller-induced distortion effect on the hydrogen-bonds around the $\text{Cu}(\text{OH}_2)_6^{2+}$ complex in solution is observable on the vibrational timescale ($\approx 10^{-13}\text{ s}$), despite the rapid reorientations of the elongation along the principal octahedral axes, ($\approx 10^{-11}\text{ s}$) [3]. The ν_{OD} wavenumbers for the two broad bands observed indicate that two groups of hydrogen bonds are formed, with mean O···O distances of about 2.74 and 2.88 \AA to the equatorial and axial water molecules, respectively.

Similar IR absorption spectra of the $\text{Cs}_2[\text{M}(\text{OH}_2)_6](\text{SO}_4)_2$ Tutton's salts with $\text{M} = \text{Cu}$ or Ni , also show a clear static Jahn–Teller effect, which splits the hydrogen bonds of the $\text{Cu}(\text{OH}_2)_6^{2+}$ ion in the solid compound into two groups of O–D-stretching frequencies with a separation of around 107 cm^{-1} . The correlation with the axial and equatorial O···O hydrogen-bond distances is satisfactory.

Acknowledgment

The Swedish Natural Science Research Council is gratefully acknowledged for financial support.

References

- [1] Bersuker I B 1984 *The Jahn–Teller Effect and Vibronic Interactions in Modern Chemistry* (New York: Plenum) ch 1–5
- [2] Perlin Yu E and Wagner M 1984 (ed.) *The Dynamical Jahn–Teller Effect in Localized Systems* (Amsterdam: North-Holland)
- [3] Poupko R and Luz Z 1972 *J. Chem. Phys.* **57** 3311
- [4] Riley M J, Hitchman M A and Mohammed A W 1987 *J. Chem. Phys.* **87** 3766
- [5] Hathaway B J 1984 *Struct. Bond.* **57** 55
- [6] Silver B J and Getz D 1974 *J. Chem. Phys.* **61** 638
- [7] Alcock N W, Duggan M, Murray A, Tyagi S, Hathaway B J and Hewat A 1984 *J. Chem. Soc. Dalton Trans.* **7**
- [8] Maslen E N, Watson K J and Moore F H 1988 *Acta Crystallogr. B* **44** 102
Maslen E N, Ridout S C and Watson K J 1988 *Acta Crystallogr. B* **44** 96
- [9] Magini M 1982 *Inorg. Chem.* **21** 1535
- [10] Ohtaki H and Maeda M 1974 *Bull. Chem. Soc. Japan* **47** 2197
- [11] Ohtaki H, Yamaguchi T and Maeda M 1976 *Bull. Chem. Soc. Japan* **49** 701
- [12] Musinu A, Paschina G, Piccaluga G and Magini M 1983 *Inorg. Chem.* **22** 1184
- [13] Tajiri Y and Wakita H 1986 *Bull. Chem. Soc. Japan* **59** 2285
- [14] Sano M, Yamatera H and Taniguchi K 1980 *Chem. Lett.* 1285
- [15] Sham T K, Hastings J B and Perlman M L 1981 *Chem. Phys. Lett.* **83** 391
- [16] Nomura M and Yamaguchi T 1988 *J. Phys. Chem.* **92** 6157
- [17] Enderby J E, Cummings S, Herdman G J, Neilson G W, Salmon P S and Skipper N 1987 *J. Phys. Chem.* **91** 5851
- [18] Neilson G W, Newsome J R and Sandström M 1981 *J. Chem. Soc. Faraday Trans. 2* **77** 1245

- [19] Salmon P S, Neilson G W and Enderby J E 1988 *J. Phys. C: Solid State Phys.* **21** 1335
- [20] Hunt J P and Friedman H L 1983 *Progr. Inorg. Chem.* **30** 359
- [21] Salmon P S, Howells W S and Mills R 1987 *J. Phys. C: Solid State Phys.* **20** 5727
- [22] Öpik U and Pryce M H L 1957 *Proc. Roy. Soc. A* **218** 450
- [23] Tamatera H 1979 *Acta Chem. Scand. Ser. A* **33** 107
- [24] Burdett J K 1981 *Inorg. Chem.* **20** 1959
- [25] Sano M and Yamatera H 1980 *Chem. Lett.* 1495
- [26] The molecule-alchemy program package incorporates the molecule integral program written by Almlöf J, and the alchemy program package (Bagus P, Liu B, Yoshimine M and MacLean D, modified by Bagus P and Wahlgren U).
- [27] Pettersson L G M, Wahlgren U and Gropen O 1983 *Chem. Phys.* **80** 7, 1987 *J. Chem. Phys.* **86** 2176
- [28] Roos B, Veillard A and Vinot G 1971 *Theor. Chim. Acta* **20** 1
- [29] Pettersson L G M and Bauschlicher C W Jr unpublished
- [30] Huzinaga S 1965 *J. Chem. Phys.* **42** 1293
- [31] Benedict W S, Gailar N and Plyler E K 1956 *J. Chem. Phys.* **24** 1139
- [32] Beagley B, Gahan B, Greaves G N and McAuliffe C A 1983 *J. Chem. Soc. Chem. Commun.* 1265
- [33] Harbron S K, Higgins S J, Levason W, Feiters M C and Steel A T 1986 *Inorg. Chem.* **25** 1789
- [34] Scott R A 1985 *Meth. Enzymol.* **117** 414
- [35] Beagley B in Hargittai I and Hargittai M (ed.) 1988 *Stereochemical Applications of Gas-Phase Electron Diffraction, Methods in Stereochemical Analysis* (New York: VCH) ch 13
- [36] Teo B K 1986 *EXAFS: Basic Principles and Data Analysis* (Berlin: Springer) ch 3
- [37] Joyner R W 1980 *Chem. Phys. Lett.* **72** 162
- [38] Kristiansson O, Eriksson A and Lindgren J 1984 *Acta Chem. Scand. Ser. A* **38** 609, 613
- [39] Kristiansson O, Lindgren J and de Villepin J 1988 *J. Phys. Chem.* **92** 2680
- [40] Enderby J E and Neilson G W 1979 in *Water, A Comprehensive Treatise* vol 6, ed. F Franks (New York: Plenum) ch 1
- [41] Berglund B, Lindgren J and Tegenfeldt J 1978 *J. Mol. Struct.* **43** 179
- [42] Shields K G and Kennard C H L 1972 *Cryst. Struct. Commun.* **1** 189
- [43] Eriksson A unpublished
- [44] Hathaway B J and Hewat A H 1984 *J. Solid State Chem.* **51** 364
- [45] Brown G M and Chidambaram R 1969 *Acta Crystallogr. B* **25** 676
- [46] Maslen E N, Ridout S C, Watson K J and Moore F H 1988 *Acta Crystallogr. C* **44** 409, 412
- [47] Montgomery H and Lingafelter E C 1965 *Acta Crystallogr.* **17** 1295